CrystEngComm

www.rsc.org/crystengcomm

Volume 15 | Number 8 | 28 February 2013 | Pages 1471–1658

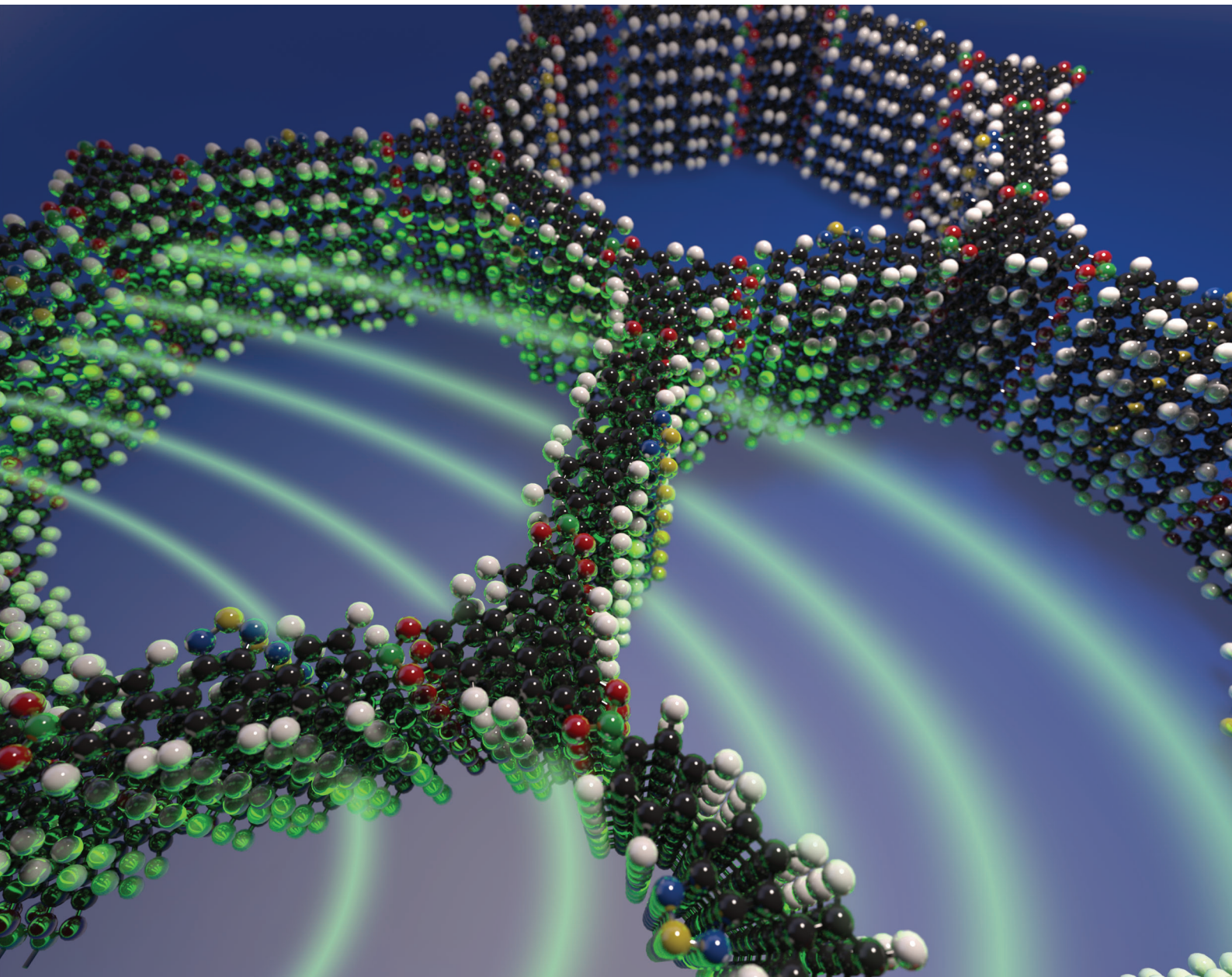

Featuring the Collection: Covalent organic frameworks

RSC Publishing

COVER ARTICLE

Paul Knochel, Thomas Bein *et al.*

Facile synthesis of a mesoporous benzothiadiazole-COF based on a transesterification process

CrystEngComm

RSC Publishing

COMMUNICATION

View Article Online
View Journal | View Issue

Facile synthesis of a mesoporous benzothiadiazole-COF based on a transesterification process†

Cite this: *CrystEngComm*, 2013, **15**, 1500

Received 21st August 2012,
Accepted 21st November 2012

DOI: 10.1039/c2ce26343b

www.rsc.org/crystengcomm

Mirjam Dogru, Andreas Sonnauer, Silvia Zimdars, Markus Döblinger, Paul Knochel* and Thomas Bein*

The synthesis of a new mesoporous BTD-COF based on a transesterification reaction was carried out in a two step microwave synthesis procedure in only 40 min: first the pinacolboronate 4,7-bis[4-(4,4,5,5)-tetramethyl-[1,3,2]dioxaborolan-2-yl)-phenyl]-benzo[1,2,5]-thiadiazole (BTDBE) was cleaved with HCl, in a second step addition of hexahydroxytriphenylene (HHTP) resulted in the growth of the crystalline framework with high surface area and a pore size of about 4 nm.

Covalent organic frameworks (COFs) are a novel class of stable, porous organic crystalline frameworks. The slightly reversible nature of the covalent bond formation reaction, for example of boronic acids with polyols, allows for the formation of ordered layers that crystallize upon condensation.[1–3] The scope of the linkage systems for 2D networks was recently expanded by reversible imine- and hydrazone-linked COFs.[4,5] In the past years COFs were mainly discussed as gas storage materials due to their light-weight frameworks with high surface areas for gas adsorption.[6–8] Moreover, catalytic activity was demonstrated with an imine-linked COF, which is capable of catalyzing Suzuki–Miyaura coupling reactions after intercalation of palladium.[9] Recently Jiang and co-workers suggested that charge carriers could be transported along the framework of COFs; they reported pyrene-containing COFs exhibiting photoconductivity and semiconducting properties.[10,11] Further evidence for high carrier mobilities was provided with the hole conducting tetragonal metallophthalocyanine COF, NiPc-COF, and the porphyrin based COFs COF-66 and COF-366.[12,13] The authors could show that by using these electroactive macrocycles as backbone building blocks it is possible to integrate properties of the monomers into the framework. Jiang and co-workers reported an n-channel COF obtained by exchanging the benzene unit in the linkers of NiPc-COF with the electron-poor benzothiadiazole (BTD) heterocyclic group.[14] These results suggest that COFs are promising materials for applications in optoelectronic devices such as OLEDs or solar cells. However, straightforward and efficient synthetic methods for COF precursors are needed to realize their potential in the above-mentioned applications. Stability issues of precursors such as the susceptibility of catechol linkers towards oxidation can be circumvented by protecting groups, such as acetyl protected alcohols. Spitler *et al.* described a Lewis acid-catalyzed COF synthesis using $BF_3{\cdot}OEt_2$ as Lewis acid and phthalocyanine tetra(acetonide) and benzenediboronic acid as building blocks.[15,16] The synthesis and use of functionalized free boronic acid monomers for COF synthesis is not very well established. Their poor solubility in organic solvents often makes the synthesis difficult and limits the exploration of a great variety of functionalized and large aromatic monomers and their incorporation into COFs. Using boronate esters as starting materials in the COF synthesis is one approach to overcome these limitations.

Here we report a general procedure for the synthesis of a boronate ester-linked COF based on a transesterification process of a boronate ester precursor. Using this approach a new mesoporous covalent organic framework, BTD-COF (Fig. 1), based on a benzothiadiazole-containing linear diboronic acid was obtained. BTD-COF was synthesized starting from 4,7-bis[4-(4,4,5,5)-tetramethyl-[1,3,2]dioxaborolan-2-yl)-phenyl]-benzo[1,2,5]-thiadiazole (BTDBE) and 2,3,6,7,10,11-hexahydroxytriphenylene (HHTP) in a two step synthesis by microwave heating.

In step 1 BTDBE was dissolved in a mixture of 1,4-dioxane and mesitylene and concentrated HCl was added. The mixture was heated up to 180 °C for 10 minutes in a microwave oven under continuous stirring (600 rpm). A phase mixture of a yellow precipitate and solvents was obtained, which was necessary for reaction step 2. HHTP and a mixture of 1,4-dioxane–mesitylene was subsequently added. The mixture was then heated in a microwave oven for 30 minutes under continuous stirring at 160 °C to finally obtain a green powder (BTD-COF) at a yield of about 75% based on BTDBE. Reference one-pot investigations for direct transesterification of BTDBE with HHTP were performed with microwave and conventional heating, but did not result in the desired BTD-COF. The optimum reaction time and temperature

Department of Chemistry and Center for NanoScience (CeNS), Ludwig-Maximilians-Universität Munich (LMU), Butenandtstraße 5-13, 81377 München Germany. E-mail: knoch@cup.uni-muenchen.de; bein@lmu.de; http://www.bein.cup.uni-muenchen.de; Fax: +49-89-2180-77622

† Electronic supplementary information (ESI) available: Synthesis procedures and structural characterization. See DOI: 10.1039/c2ce26343b

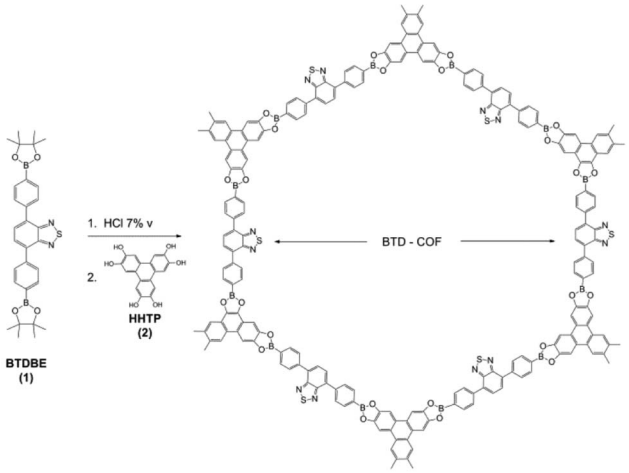

Fig. 1 Illustration of the reaction pathway towards BTD-COF.

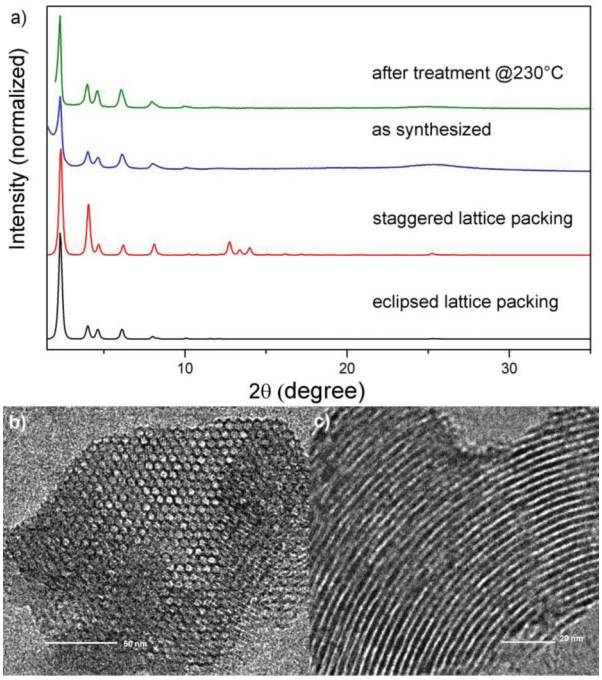

Fig. 2 (a) PXRD pattern of BTD-COF after guest removal at 230 °C for 12 h (green) and BTD-COF as synthesized (blue) compared to the simulated PXRD pattern in AA arrangement (black) and AB arrangement (red). Transmission electron micrographs of BTD-COF, (b) projection along the columns showing the hexagonal structure, (c) image of a crystal tilted out of the columnar projection with a side view of the pores. Scale bars: 50 nm and 20 nm, respectively

for each of the two steps were optimized by systematic parameter screening. The evaluation was based on the crystallinity and yield of the obtained BTD-COF (Fig. S1, ESI†).

Based on the functional groups and the geometry of the used precursor molecules, the final structure can be predicted and then compared to the experimental powder X-ray diffraction pattern (PXRD). According to the geometry and connectivity of the precursor molecules, a two-dimensional layered structure with hexagonal symmetry is expected. In principle a staggered and an eclipsed arrangement of the hexagonal sheets is possible. Geometry optimizations of both crystal structures based on universal force field methods were performed and the diffraction patterns for both arrangements were simulated (Fig. S2–S6, ESI†). In Fig. 2a the simulated PXRD-patterns are compared to the experimentally obtained data, indicating an eclipsed arrangement, due to the disagreement with the staggered conformation and a good agreement with the eclipsed lattice packing. The BTD-COF shows X-ray diffraction (XRD) peaks at 2.30, 4.99, 4.63, 6.13, 7.98 and 25.5° 2θ, corresponding to the (100), (110), (200), (210), (300), and (001) lattice orientations, respectively.

Transmission electron microscopy shows a crystalline material with domains of about 100 nm in size. In Fig. 2b, the TEM image shows the periodic hexagonal structure with a pore-to-pore distance of about 3.8 nm. The crystal structure parameters *a* and *b* obtained from PXRD (4.3 nm) match very well the calculations (4.2 nm). These values agree with the data obtained by TEM taking into account a possible shrinkage due to ultra high vacuum and electron beam exposure. In Fig. 2c a view along the pores is given, indicating extended and open channels in the structure.

Nitrogen sorption measurements revealed the porosity of the BTD-COF framework after degassing the sample at 230 °C for 12 h. The adsorption isotherm was recorded at 77 K. BTD-COF exhibits a type IV isotherm (Fig. 3a) typical for mesoporous materials,[17] and a Brunauer Emmett Teller (BET) surface area of 1000 $m^2\ g^{-1}$. The sharp step in the isotherm indicates a very narrow pore size distribution, which is reflected in the size distribution around 4.1 nm obtained from NLDFT calculations (Fig. 3b). The experimental pore size agrees very well with the theoretically predicted one of 4.2 nm (arithmetic average of the pore sizes of the long and short axes of the hexagons).

FT-IR spectroscopy confirmed the presence of the boronate ester functionality of BTD-COF (Fig. S8, ESI†). Comparison of the ^{11}B MAS NMR spectra (Fig. S9, ESI†) of the starting material

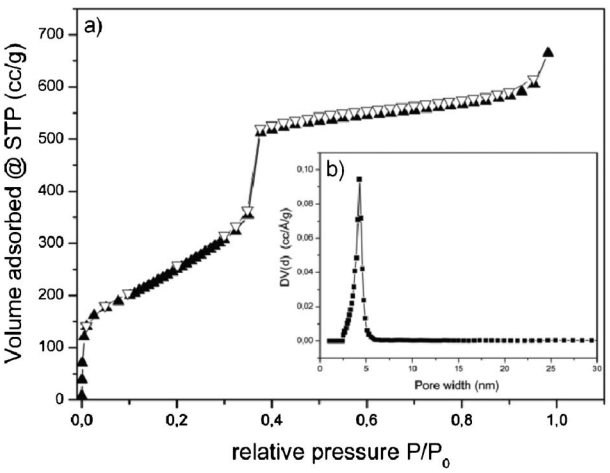

Fig. 3 (a) Nitrogen sorption isotherm of degassed BTD-COF measured at 77 K and (b) pore size distribution with a mean pore size of about 4.1 nm.

Published on 22 November 2012.

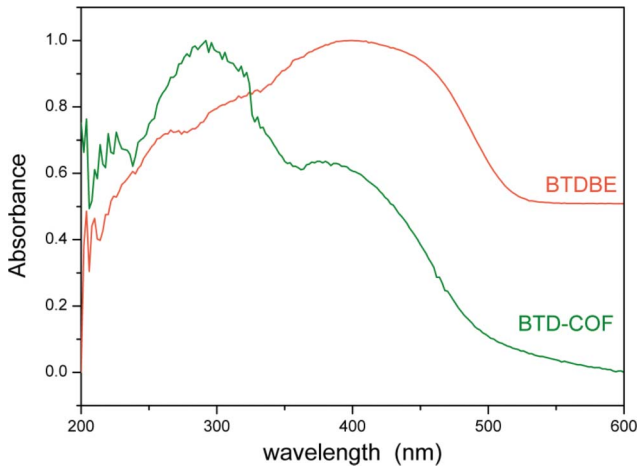

Fig. 4 UV-vis absorbance spectrum of BTD-COF (green) and the starting pinacol ester (orange).

BTDBE with BTD-COF shows almost identical chemical shifts. BTDBE is an aliphatic boronate ester with a chemical shift of 23.7 ppm, and the resonance of the aromatic boronate ester BTD-COF occurs at 22.2 ppm.

^{13}C CP-MAS-NMR confirmed the transesterification reaction during the framework formation, which is reflected in the absence of the signals of the methyl groups of the starting pinacol ester. Signals from both building blocks are present and can be assigned to their carbon atoms (Fig. S10, ESI†). Thermogravimetric analysis (Fig. S11, ESI†) indicates that BTD-COF decomposes above 450 °C.

The absorbance spectrum (Fig. 4) of the BTD-COF shows broad features between 250 nm and 500 nm, with two maxima at 300 nm and 400 nm. Jiang and co-workers assigned the second maximum to a charge transfer from the electron-donating HHTP moiety to the electron-accepting BTD moiety.[18] An electronic bandgap of 2.48 eV was calculated from the spectrum. The fluorescence spectra (Fig. S12, ESI†) show fluorescence quenching in BTD-COF, which is attributed to internal energy transfer from the electron donating HHTP moieties to the electron accepting BTD in the COF lattice.[19,20]

In conclusion, the use of a boronate ester instead of a free boronic acid improves the solubility of the COF-precursors, and thus facilitates the synthesis of COF structures. The 2-step microwave-assisted synthesis pathway reported here allowed us to simplify and accelerate the boronate ester-based COF synthesis. Using this approach, we could synthesize a 2D eclipsed BTD-COF structure. Condensation of a benzothiadiazole-functionalized terphenyl diboronic acid ester with HHTP gives a crystalline framework with large accessible pores within only 40 min. Investigation of the structure with TEM confirms the lattice characteristics obtained from theoretical simulations and X-ray diffraction data. BTD-COF is a highly thermally and chemically stable material, which can be handled under ambient conditions and shows resistance against most common organic solvents.

Published on 22 November 2012.

Acknowledgements

We gratefully acknowledge financial support from the NIM excellence cluster (DFG).

References

1 A. P. Côté, A. I. Benin, N. W. Ockwig, M. O'Keeffe, A. J. Matzger and O. M. Yaghi, *Science*, 2005, **310**, 1166–1170.
2 A. P. Côté, H. M. El-Kaderi, H. Furukawa, J. R. Hunt and O. M. Yaghi, *J. Am. Chem. Soc.*, 2007, **129**, 12914–12915.
3 R. W. Tilford, W. R. Gemmill, H.-C. zur Loye and J. J. Lavigne, *Chem. Mater.*, 2006, **18**, 5296–5301.
4 F. J. Uribe-Romo, J. R. Hunt, H. Furukawa, C. Klöck, M. O'Keeffe and O. M. Yaghi, *J. Am. Chem. Soc.*, 2009, **131**, 4570–4571.
5 F. J. Uribe-Romo, C. J. Doonan, H. Furukawa, K. Oisaki and O. M. Yaghi, *J. Am. Chem. Soc.*, 2011, **133**, 11478–11481.
6 S. S. Han, H. Furukawa, O. M. Yaghi and W. A. Goddard III, *J. Am. Chem. Soc.*, 2008, **130**, 11580–11581.
7 C. J. Doonan, D. J. Tranchemontagne, T. G. Glover, J. R. Hunt and O. M. Yaghi, *Nat. Chem.*, 2010, **2**, 235–238.
8 H. Furukawa and O. M. Yaghi, *J. Am. Chem. Soc.*, 2009, **131**, 8875–8883.
9 S.-Y. Ding, J. Gao, Q. Wang, Y. Zhang, W.-G. Song, C.-Y. Su and W. Wang, *J. Am. Chem. Soc.*, 2011, **133**, 19816–19822.
10 S. Wan, J. Guo, J. Kim, H. Ihee and D. Jiang, *Angew. Chem., Int. Ed.*, 2008, **47**, 8826–8830.
11 S. Wan, J. Guo, J. Kim, H. Ihee and D. Jiang, *Angew. Chem., Int. Ed.*, 2009, **48**, 5439–5442.
12 X. Ding, J. Guo, X. Feng, Y. Honsho, J. Guo, S. Seki, P. Maitarad, A. Saeki, S. Nagase and D. Jiang, *Angew. Chem., Int. Ed.*, 2011, **50**, 1289–1293.
13 S. Wan, F. Gándara, A. Asano, H. Furukawa, A. Saeki, S. K. Dey, L. Liao, M. W. Ambrogio, Y. Y. Botros, X. Duan, S. Seki, J. F. Stoddart and O. M. Yaghi, *Chem. Mater.*, 2011, **23**, 4094–4097.
14 X. Ding, L. Chen, Y. Honsho, X. Feng, O. Saengsawang, J. Guo, A. Saeki, S. Seki, S. Irle, S. Nagase, V. Parasuk and D. Jiang, *J. Am. Chem. Soc.*, 2011, **133**, 14510–14513.
15 E. L. Spitler and W. R. Dichtel, *Nat. Chem.*, 2010, **2**, 672–677.
16 E. L. Spitler, M. R. Giovino, S. L. White and W. R. Dichtel, *Chem. Sci.*, 2011, **2**, 1588–1593.
17 S. Kitagawa, R. Kitaura and S.-I. Noro, *Angew. Chem., Int. Ed.*, 2004, **43**, 2334–2375.
18 X. Feng, L. Chen, Y. Honsho, O. Saengsawang, L. Liu, L. Wang, A. Saeki, S. Irle, S. Seki, Y. Dong and D. Jiang, *Adv. Mater.*, 2012, **24**, 3026–3031.
19 E. E. Neuteboom, P. A. van Hal and R. A. J. Janssen, *Chem.–Eur. J.*, 2004, **10**, 3907–3918.
20 Q. Zhang, A. Cirpan, T. P. Russell and T. Emrick, *Macromolecules*, 2009, **42**, 1079–1082.